Modulation of cell-cycle dynamics is required to regulate the number of cerebellar GABAergic interneurons and their rhythm of maturation

Development 138, 3463-3472 (2011) doi:10.1242/dev.064378

Modulation of cell-cycle dynamics is required to regulate the number of cerebellar GABAergic interneurons and their rhythm of maturation

Ketty Leto[1,2], Alice Bartolini[1,2], Alessandra Di Gregorio[1,2], Daniele Imperiale[3], Annarita De Luca[1,2], Elena Parmigiani[1,2], Robert K. Filipkowski[4], Leszek Kaczmarek[5] and Ferdinando Rossi[1,2,*]

SUMMARY

The progenitors of cerebellar GABAergic interneurons proliferate up to postnatal development in the prospective white matter, where they give rise to different neuronal subtypes, in defined quantities and according to precise spatiotemporal sequences. To investigate the mechanisms that regulate the specification of distinct interneuron phenotypes, we examined mice lacking the G1 phase-active cyclin D2. It has been reported that these mice show severe reduction of stellate cells, the last generated interneuron subtype. We found that loss of cyclin D2 actually impairs the whole process of interneuron genesis. In the mutant cerebella, progenitors of the prospective white matter show reduced proliferation rates and enhanced tendency to leave the cycle, whereas young postmitotic interneurons undergo severe delay of their maturation and migration. As a consequence, the progenitor pool is precociously exhausted and the number of interneurons is significantly reduced, although molecular layer interneurons are more affected than those of granular layer or deep nuclei. The characteristic inside-out sequence of interneuron placement in the cortical layers is also reversed, so that later born cells occupy deeper positions than earlier generated ones. Transplantation experiments show that the abnormalities of cyclin D2$^{-/-}$ interneurons are largely caused by cell-autonomous mechanisms. Therefore, cyclin D2 is not required for the specification of particular interneuron subtypes. Loss of this protein, however, disrupts regulatory mechanisms of cell cycle dynamics that are required to determine the numbers of interneurons of different types and impairs their rhythm of maturation and integration in the cerebellar circuitry.

KEY WORDS: Cyclin D2, Neuronal specification, Neurogenesis, Cerebellum, Mouse

INTRODUCTION

The different types of GABAergic interneurons of the cerebellar cortex and nuclei derive from a common pool of multipotent progenitors (Leto et al., 2006), which upregulate the transcription factor Pax2 during their last mitosis (Weisheit et al., 2006; Leto et al., 2009). These progenitors originate from the medial region of the cerebellar ventricular neuroepithelium (VN) (Mizuhara et al., 2010), but delaminate to the prospective white matter (PWM), where they continue to divide up to postnatal development (Zhang and Goldman, 1996; Maricich and Herrup, 1999; Milosevic and Goldman, 2002). Different interneuron populations are generated in the PWM according to a precise inside-out positional sequence, in which cell identity and laminar placement are temporally related to the neuron birthdate. Fate choices, however, are not definitively established in dividing progenitors, and postmitotic cells exposed to heterochronic environments are still able to acquire host-specific interneuron identities (Leto et al., 2009).

This peculiar mechanism that creates a variety of phenotypes from a single source implies that the PWM provides spatiotemporally patterned instructive signals to generate different neuronal categories at defined developmental stages. Furthermore, the different interneuron phenotypes must be produced in precise quantities: for each interneuron of the cerebellar nuclei there are about 35 Golgi cells, and 950 basket and stellate neurons (Altman and Bayer, 1997). Nevertheless, the mechanisms that determine the specification and regulate the numbers of cerebellar GABAergic interneurons remain unclear.

Several studies indicate that defects of cell cycle regulation significantly influence the differentiation of specific neuron populations (Glickstein et al., 2007b; Sakagami et al., 2009; Lee et al., 2010). In particular, mice that lack the G1 phase-active protein cyclin D2 (Ccnd2) show a hypomorphic cerebellum, with a reduced number of granule neurons and virtually no stellate cells, whereas other types of GABAergic interneurons are preserved (Huard et al., 1999). The selective lack of one class of interneurons suggests that cyclin D2 could be required for the specification of this phenotype. Alternatively, however, as stellate cells are the latest interneurons generated during cerebellar ontogenesis, their absence could reflect a premature exhaustion of the progenitor pool. To discriminate between these possibilities, we have compared the genesis of GABAergic interneurons in wild-type and *Ccnd2*$^{-/-}$ cerebella. We show that lack of cyclin D2 actually impairs the production of all interneuron categories. In mutant cerebella, mitotic activity of PWM progenitors is dramatically reduced and the differentiation of GABAergic interneurons is considerably delayed. Furthermore, transplantation of *Ccnd2*$^{-/-}$ cells to wild-type cerebella (and vice versa) shows that these abnormalities are due to cell-autonomous mechanisms. Therefore, loss of cyclin D2 does not impair the acquisition of specific interneuron phenotypes, but severely disrupts the whole process of interneuron genesis and maturation.

[1]Neuroscience Institute of Turin (NIT), Department of Neuroscience, University of Turin, I-10125 Turin, Italy. [2]Neuroscience Institute of the Cavalieri-Ottolenghi Foundation (NICO), University of Turin, Regione Gonzole 10, 10043 Orbassano Turin, Italy. [3]Maria Vittoria Hospital, Division of Neurology, 10144 Turin, Italy. [4]University of Finance and Management in Warsaw, Department of Biological Psychology, 55 Pawia St, 01-030 Warsaw, Poland. [5]Nencki Institute of Experimental Biology, 3 Pasteur str., 02-093 Warsaw, Poland.

*Author for correspondence (ferdinando.rossi@unito.it)

Accepted 13 June 2011

MATERIALS AND METHODS

Animals and surgical procedures

Homozygous cyclin D2-null mice [originally produced by Sicinski et al. (Sicinski et al., 1996)] are infertile and the line was maintained in heterozygosis after backcrossing into C57BL/6 background over ten times. *Ccnd2*$^{+/-}$ mice were bred to produce wild-type and homozygous null littermates. Genomic DNA was extracted from tail snips using standard protocols and examined by PCR-based genotyping using primers for wild-type and null alleles (Sicinski et al., 1995; Sessa et al., 2008). Heterozygous *Ccnd2*$^{+/-}$ mice were also crossbred with Pax2/GFP mice (Pfeffer et al., 2002), in which the reporter is selectively expressed in all cerebellar interneurons up to adulthood (Weisheit et al., 2006). Wild-type recipients in transplantation experiments were C57BL/6 mice.

Surgical procedures were performed under deep general anaesthesia obtained by intraperitoneal administration of ketamine (100 mg/kg; Ketavet, Bayer) supplemented by xylazine (5 mg/kg; Rompun, Bayer) or diazepam (2.5 mg/kg; Roche). The experimental plan was designed according to the European Communities Council Directive (86/609/EEC), the NIH guidelines and the Italian law for care and use of experimental animals (DL116/92), and was approved by the Italian Ministry of Health and the Ethical Committee at the University of Turin.

Transplantation experiments

Donor cells were isolated from Pax2/GFP wild-type or *Ccnd2*$^{-/-}$ mice of different ages and grafted to wild-type or mutant cerebella (see Table S2 in the supplementary material), as described (Jankovski et al., 1996; Carletti et al., 2002). A single-cell suspension (1 μl at a final concentration 5×10^4 cells/μl), obtained by mechanical dissociation of embryonic cerebellar primordia or of postnatal cerebella, was pressure-injected through a glass capillary into the cerebella of recipient mice.

Histological procedures

Under deep general anaesthesia, the mice were transcardially perfused with 250 ml of 4% paraformaldehyde in 0.12 M phosphate buffer (pH 7.2-7.4). The brains were immediately dissected, postfixed overnight at 4°C and transferred to 30% sucrose in 0.12 M phosphate buffer. The cerebella were cut in 30 μm parasagittal cryostat sections. Immunofluorescent staining of wild-type and mutant sections was performed in parallel to minimize inter-experiment variability. Primary antibodies were dissolved in PBS, with 1.5% normal serum and 0.25% Triton X-100, and incubated overnight at 4°C with: anti-parvalbumin (1:1500, Swant), anti-Pax2 (1:200, Zymed), anti-calbindin (1:1500, Swant); anti-Ki67 (1:1000, Abcam); anti-GFP (1:700, Invitrogen), anti-BrdU (1:500, Sigma); anti-caspase 3 (1:200, Euroclone) or anti-Sox2 (1:1500, Chemicon). The sections were exposed for 1 hour at room temperature to fluoresceinated second antibodies (1:200; Vector) or biotinylated secondary antibodies followed by streptavidin-Texas Red conjugate (1:200; Invitrogen). 4′,6′-diamidino-2-phenylindole (DAPI, Fluka) was used to counterstain cell nuclei. For BrdU immunostaining, the sections were incubated in 2 N HCl for 20 minutes at 37°C, exposed to anti-BrdU antibodies (1:500, Sigma) overnight at 4°C and reacted with fluoresceinated second antibody. The stained sections were mounted in Tris-glycerol supplemented with 10% Mowiol (Calbiochem).

For immunocytochemical labelling of cyclins, fixed cerebella were embedded in paraffin wax and cut in 5 μm sections, which were treated with 3% H_2O_2 for 10 minutes and incubated overnight at 4°C with anti-cyclin D1 (1:500, LabVision) or anti-cyclin D2 (1:500, LabVision) antibodies. The sections were incubated with secondary antibodies followed by the Vectastain Elite kit (Vector Laboratories) for 30 minutes each, and finally revealed by reaction with 3,3′-diaminobenzidine. The sections were counterstained with Haematoxylin, dehydrated and coverslipped.

Morphometric and quantitative analyses

Histological specimens were examined using a Leica DM 6000 CS confocal microscope. Quantitative and morphometric evaluations were made using the Neurolucida software (MicroBrightField) connected to an E-800 Nikon microscope via a colour CCD camera or using ImageJ programme (Research Service Branch, NIH; http://rsb.info.nih.gov/ij/).

All quantifications were performed blind to genotype on reconstructions of the entire E15 cerebellar primordium or of lobules IV/V of postnatal cerebella, obtained by combining confocal images (1-3 μm, 40× magnification). Usually, three sections per individual were examined and the obtained data were averaged. All groups contained sets of wild-type and *Ccnd2*$^{-/-}$ littermates, and tissues derived from three or more litters were examined for each parameter. In embryonic cerebella, the SVZ was defined as the region between the VN and nascent cortical plate. In postnatal animals, the PWM was the region surrounding the DCN and extended along the axis of cortical folia, up to the inner GL border.

The number of interneurons/mm^2 was counted over the entire cortical lobules IV/V or DCN region in four to seven animals per group at P30 (at least three sections/animal; 981 cells from *Ccnd2*$^{-/-}$ mice, 9834 cells from wild-type mice). Both ectopic and correctly positioned neurons were counted and reported in the histograms. The perikaryal size of the sampled neurons was measured with Neurolucida on samples of 120 cells from at least four mice/genotype. The obtained values of neuronal density were corrected by applying the Abercrombie formula (Abercrombie, 1946) to compensate for size differences in wild-type and mutant animals.

To determine the birthdates of ML interneurons, single intraperitoneal injections of BrdU (50 μg/g body weight, dissolved at 5 mg/ml in 0.007 N NaOH in saline) were administered to P1, P5 or P10 mice (for each time point several hundred cells were sampled from three to six cases). For GL and DCN interneuron birthdating, single doses of BrdU were injected to pregnant E15 dams or postnatal pups (P1 or P5) of Pax2/GFP and Pax2/GFP/*Ccnd2*$^{-/-}$ mice. The animals were killed at P30. The laminar distribution of BrdU-labelled cells was determined as described by Leto et al. (Leto et al., 2009) (at least 50 cells/case, three cases/age group). Briefly, the position of each cell was recorded as the distance from the Purkinje cell layer (positive for the ML, negative for the GL). Raw measurements were normalized relative to the layer thickness and represented as scatter diagrams, in which samples from different mice of the same set were pooled together.

The number of Pax2-positive nuclei/mm^2 was evaluated in the SVZ of E15 embryos (three sections/case, n=4 wild type, n=7 *Ccnd2*$^{-/-}$), or in the PWM of P1 or P5 pups (three sections/case, n=6 wild type, n=4 *Ccnd2*$^{-/-}$ at both ages). For each time point, 200-800 labelled nuclei were sampled from wild-type and mutant cerebella.

To investigate the proliferation and initial maturation of cerebellar interneurons, single BrdU pulses were injected to P3 wild-type and *Ccnd2*$^{-/-}$ mice, which were killed after 2 hours (n=5 wild type, n=3 *Ccnd2*$^{-/-}$), 24 hours (n=3 per genotype), 72 hours (n=3 per genotype), 5 days (n=4 wild type, n=2 *Ccnd2*$^{-/-}$) or 8 days (n=3 wild type, n=2 *Ccnd2*$^{-/-}$). On vermal sections double-immunolabelled for BrdU and Pax2, we evaluated the density (cell/mm^2) and recorded the position of single and double-labelled nuclei in the PWM or in the cortical layers of lobules IV/V (three or four cases/time point/genotype). The total number of double-labelled cells counted in wild-type mice was 137 at 2 hours, 429 at 24 hours and 1091 at 72 hours; in mutant mice, it was 50 cells at 72 hours (Fig. 5B,C). The same procedure was applied to assess the distribution of cells double-labelled for BrdU and GFP in Pax2/GFP and Pax2/GFP*Ccnd2*$^{-/-}$ cerebella (two or three cases/age group/genotype). Cell death was estimated by counting caspase 3-immunopositive cells in the PWM at P1 and P5 (five sections/case, three cases/age/genotype).

To evaluate Pax2 expression level in young postmitotic interneurons, we measured the intensity of GFP fluorescence in BrdU-retaining cells in the PWM of Pax2/GFP or Pax2/GFP/*Ccnd2*$^{-/-}$ mice, 72 hours after BrdU pulse. Green-fluorescence intensity, which is related to the level of Pax2 protein expression (Weisheit et al., 2006), was measured by means of neurolucida on single confocal sections (48 cells/three wild-type mice, 50 cells/four *Ccnd2*$^{-/-}$ mice) (Leto et al., 2009).

To investigate cell cycle dynamics, BrdU was administered to E15 pregnant dams and P1 and P5 postnatal pups either 2 or 24 hours before harvest in order to evaluate the pool of dividing progenitors, the S-phase index and the proliferative fraction, as described in the Results (three to five cases/age group for both wild-type and *Ccnd2*$^{-/-}$ mice, several hundred cells for each staining and each group) (Glickstein et al., 2009).

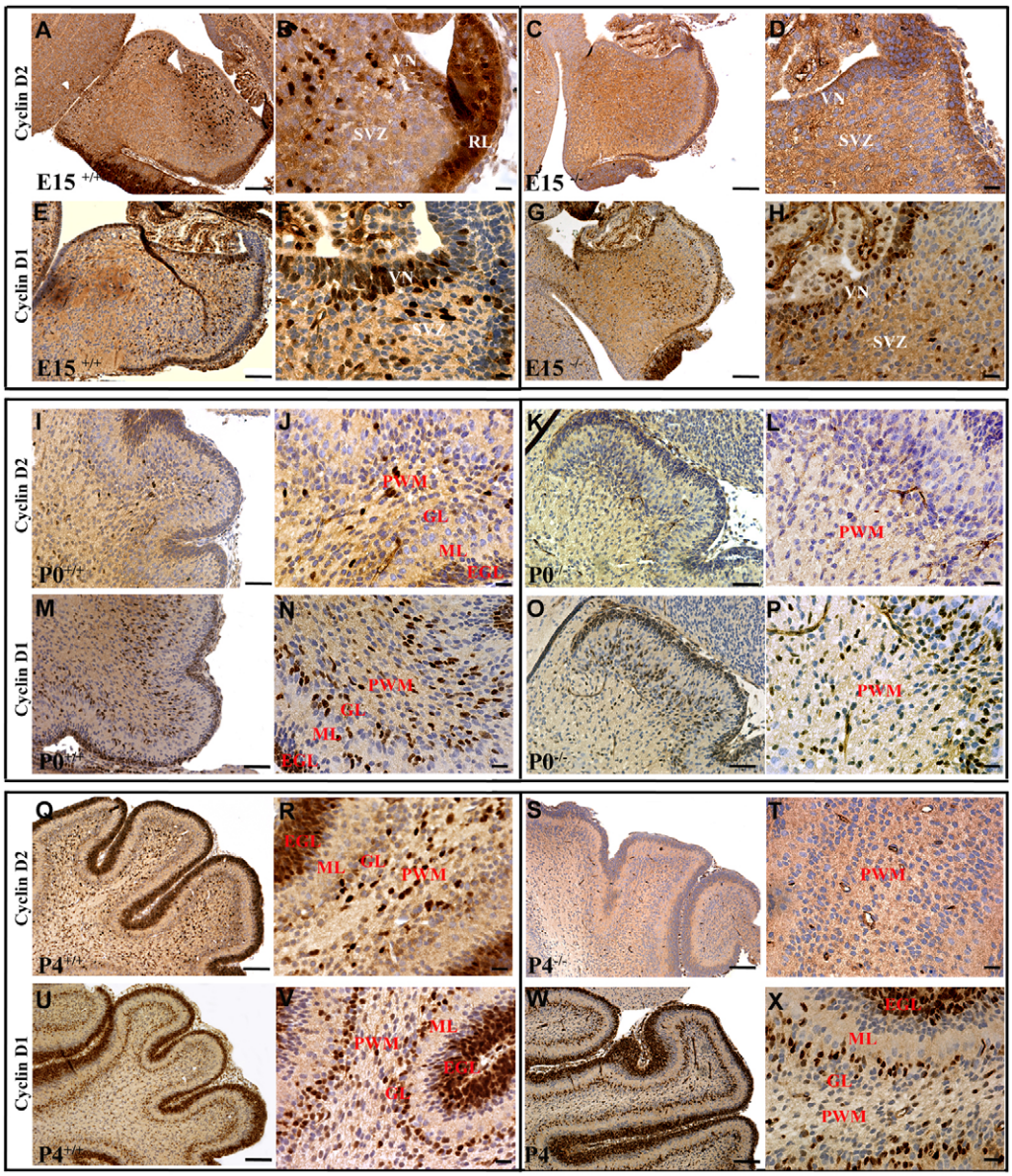

Fig. 1. Expression of D-type cyclins during cerebellar development. (**A-H**) Distribution of cyclin D2 (A-D) and cyclin D1 (E-H) in the E15 cerebellum of wild-type (A,B,E,F) and *Ccnd2*$^{-/-}$ (C,D,G,H) mice. In wild-type mice, most *Ccnd2*-expressing cells are located in the SVZ (A,B), whereas cyclin D1-positive nuclei are packed in the VN (E,F). In mutant cerebella, cyclin D2 is absent (C,D), whereas cyclin D1 localization is unchanged (G,H). (**I-P**) Expression of the two cyclins in P0 wild-type (I,J,M,N) and *Ccnd2*$^{-/-}$ (K,L,O,P) cerebella. In wild-type mice, cyclin D2-positive cells are present in the PWM (I,J). Cyclin D1 immunolabelled nuclei are sparse in the PWM, but frequent in the GL (M,N). Both cyclins are expressed in the EGL. In mutant mice, cyclin D2 is absent (K,L), whereas the distribution of cyclin D1 is unaltered (O,P). (**Q-X**) A similar expression pattern of both proteins is observed at P4 in wild-type (Q,R,U,V) and *Ccnd2*$^{-/-}$ (S,T,W,X) cerebella. VN, ventricular neuroepithelium; SVZ, subventricular zone; EGL, external granular layer; ML, molecular layer; GL, granular layer; PWM, prospective white matter. Scale bars: 200 μm in A,C,E,G,I,K,M,O,Q,S,U,W; 100 μm in B,D,F,H,J,L,N,P,R,T,V,X.

Analysis of transplanted interneurons

Donor cells in the host tissue were recognized by GFP expression. Phenotypes were identified according to morphological features and expression of type-specific markers (Leto et al., 2006). The same procedures described above were applied to measure the size and record the positions of donor interneurons in the recipient cerebella. Results obtained from different cases belonging to the same experimental set were usually pooled together.

Statistical analysis

Statistical significance was assessed by unpaired Student's *t*-test when two groups were analyzed. When three or more groups were considered, one-way ANOVA with Bonferroni's Multiple Comparisons Test was used; $P<0.05$ was considered to be statistically significant.

RESULTS

Expression of D-type cyclins during cerebellar development

To elucidate the role of cyclin D2 in the genesis of cerebellar GABAergic interneurons, we first examined the expression patterns of cyclin D2 and cyclin D1 in wild-type and *Ccnd2*$^{-/-}$ mice at E15, P0 and P4 (Fig. 1). In wild-type embryos, the two proteins displayed a reciprocal distribution: most cyclin D1-labelled nuclei were densely packed in the VN (Fig. 1E,F), whereas cyclin D2-expressing cells were almost exclusively found in the subventricular zone (SVZ, Fig. 1A,B), the domain where Pax2-positive GABAergic interneurons are initially found (Maricich and Herrup, 1999; Zordan et al., 2008). Both cyclins were expressed in the rhombic lip (Fig. 1A,B,E,F), which is the origin of glutamatergic cerebellar neurons (Machold and Fishell, 2005; Wang et al., 2005). In mutant embryos, there was no cyclin D2 labelling (Fig. 1C,D), but cyclin D1 retained the same expression pattern of wild-type cerebella (Fig. 1G,H).

In wild-type cerebella at P0 (Fig. 1I-P) or P4 (Fig. 1Q-X), cyclin D2-positive cells were mostly localized in the PWM (Fig. 1I,J,Q,R). Cyclin D1-positive nuclei were primarily aligned along a thin cellular rim immediately below the row of Purkinje cell perikarya (Fig. 1M,N,U,V). Both cyclins were expressed in the external granular layer (EGL, Fig. 1I,M,Q,U). In age-matched mutant mice, cyclin D2 staining was virtually absent, whereas cD1 expression retained the same distribution of wild-type cerebella

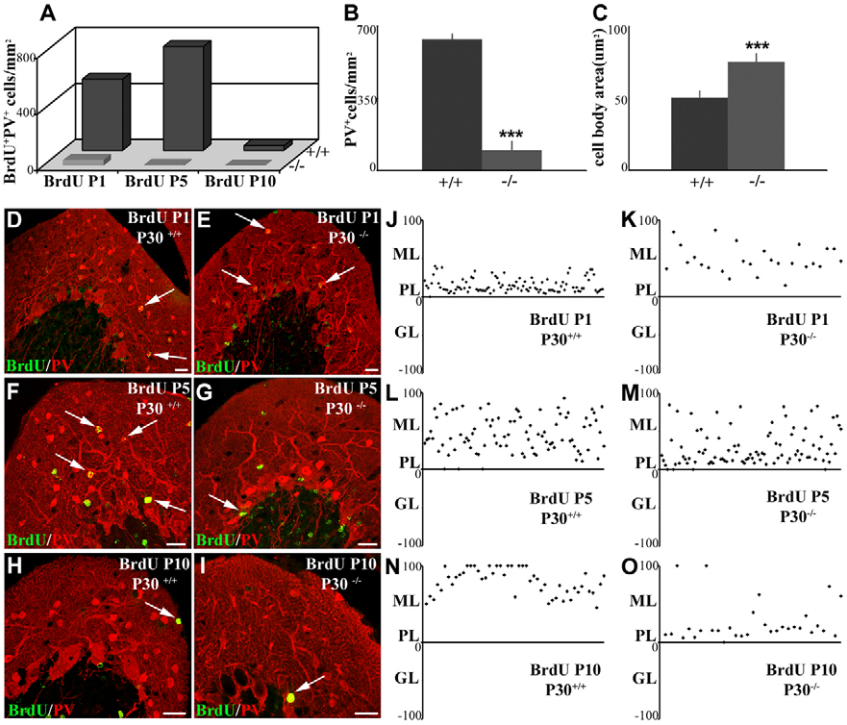

Fig. 2. Reduced number and reverse laminar placement of *Ccnd2*$^{-/-}$ ML interneurons. (**A**) Frequencies of ML interneurons double-labelled for BrdU and PV in P30 wild-type and *Ccnd2*$^{-/-}$ mice that received BrdU injection at P1, P5 or P10. (**B**,**C**) At P30, the density of PV-positive interneurons, including both correctly positioned and ectopic cells, is reduced (B), whereas their perikaryal size is increased (C). Data are mean+s.d. Student's *t*-test, ***P<0.0001. (**D-I**) Cerebellar sections of P30 wild-type (D,F,H) and *Ccnd2*$^{-/-}$ mice (E,G,I). Arrows indicate cells that are double-labelled for PV (red) and BrdU (green) after BrdU administration at P1 (D,E), P5 (F,G) and P10 (H,I; see individual channels in Fig. S1 in the supplementary material). (**J-O**) Laminar position of PV-immunopositive ML interneurons that incorporated BrdU at P1 (J,K), P5 (L,M) and P10 (N,O) in P30 wild-type (J,L,N) and *Ccnd2*$^{-/-}$ (K,M,O) mice. Note the inverted outside-in positional gradient of interneuron generation in *Ccnd2*$^{-/-}$ cerebella. ML, molecular layer; PL, Purkinje cell layer; GL, granular layer. Scale bars: 20 μm in D-I.

(Fig. 1O,P,W,X). At all ages, the frequency of cyclin D1-positive nuclei in the SVZ or PWM was not different in *Ccnd2*$^{-/-}$ or wild-type mice (see Table S1 in the supplementary material), showing that loss of cyclin D2 was not compensated by upregulation of cyclin D1.

Lack of cyclin D2 impairs the production and placement of all types of cerebellar GABAergic interneurons

To determine whether cyclin D2 function is required to generate stellate neurons but not other types of cerebellar interneurons (Huard et al., 1999), we evaluated the frequencies of the different interneuron phenotypes and their laminar distribution in relation to cell birthdates. We first examined interneurons of the molecular layer (ML; basket and stellate cells), which are specifically labelled by anti-parvalbumin antibodies (PV) (Celio, 1990; Bastianelli, 2003). As ML interneurons are primarily generated during postnatal development (Altman and Bayer, 1997), wild-type and *Ccnd2*$^{-/-}$ mice received single pulses of bromodeoxyuridine (BrdU) at P1 (Fig. 2A,D,E), P5 (Fig. 2A,F,G) and P10 (Fig. 2A,H,I; n=3/4 cases for each genotype/age), and were examined at P30. At all ages of BrdU administration, the amount of ML interneurons double-labelled for PV and BrdU was dramatically lower in mutant than in wild-type cerebella (Fig. 2A). Accordingly, the density of PV-immunopositive interneurons in *Ccnd2*$^{-/-}$ P30 mice was reduced by about 80% (Fig. 2B; Student's *t*-test, P<0.0001, n=4 for both sets), but their perikarya were significantly oversized (Fig. 2C; Student's *t*-test, P<0.0001). In the mutant cerebella, PV immunostaining revealed the typical basket axon pinceaux surrounding Purkinje cell somata. PV-immunopositive interneurons, however, were distributed throughout the ML (Fig. 1E,G,I,K,M,O; see Fig. S1 in the supplementary material), suggesting that both basket and stellate cells were present. This conclusion was confirmed by examination of Pax-2-GFP/*Ccnd2*$^{-/-}$ mice (not shown), in which all cerebellar interneurons are green fluorescent, and also by the analysis of transplantation experiments (Fig. 7B,C).

In wild-type cerebella, the laminar position of ML interneurons born at different ages revealed the typical inside-out sequence (Fig. 1J,L,N) (Leto et al., 2009). Surprisingly, this sequence was reversed in *Ccnd2*$^{-/-}$ cerebella, where the placement of ML interneurons followed an outside-in progression (Fig. 2K,M,O; Student's *t*-test, P<0.0001 for the position of cells born at P1 and P10 in wild-type versus *Ccnd2*$^{-/-}$ mice; P=0.01 for cells born at P5). As a consequence, *Ccnd2*$^{-/-}$ ML interneurons generated at P10 were fated toward the same positions as their wild-type counterparts born at P1 (compare Fig. 2J,O; Student's *t*-test, P=0.17).

To analyze interneurons of the granular layer (GL, Golgi and Lugaro cells) and of the deep cerebellar nuclei (DCN), we examined Pax2-GFP/*Ccnd2*$^{-/-}$ mice. As these interneurons are mostly generated during late embryonic/early postnatal life (Altman and Bayer, 1997), the mice received BrdU pulses at E15, P1 or P5, and were examined at P30 (Fig. 3). In *Ccnd2*$^{-/-}$ mice, GL interneurons were significantly reduced by about 25% (Fig. 3A,E,I; Student's *t*-test, P<0.01, n=4 *Ccnd2*$^{-/-}$ mice, n=7 wild-type mice), whereas DCN interneurons were reduced by about 60% (Fig. 3C,G,K; Student's *t*-test, P<0.0001). Furthermore, mutant interneurons had significantly larger perikarya than their wild-type counterparts (GL interneurons, Fig. 3B,F,J; Student's *t*-test, P<0.01; DCN interneurons, Fig. 2D,H,L, Student's *t*-test, P<0.001). Evaluation of the laminar position of GL interneurons again revealed a reverse outside-in sequence in the mutant cerebella, where cells born at E15 adopted more superficial positions than those born at P1 (Fig. 3M-P; Student's *t*-test, P<0.0001, for the position of both E15 and P1 generated cells, wild-type versus *Ccnd2*$^{-/-}$ mice). BrdU pulsed at P5 yielded some labelled nuclei in the GL of wild-type animals, but not in *Ccnd2*$^{-/-}$ mice, suggesting a precocious exhaustion of GL interneuron production.

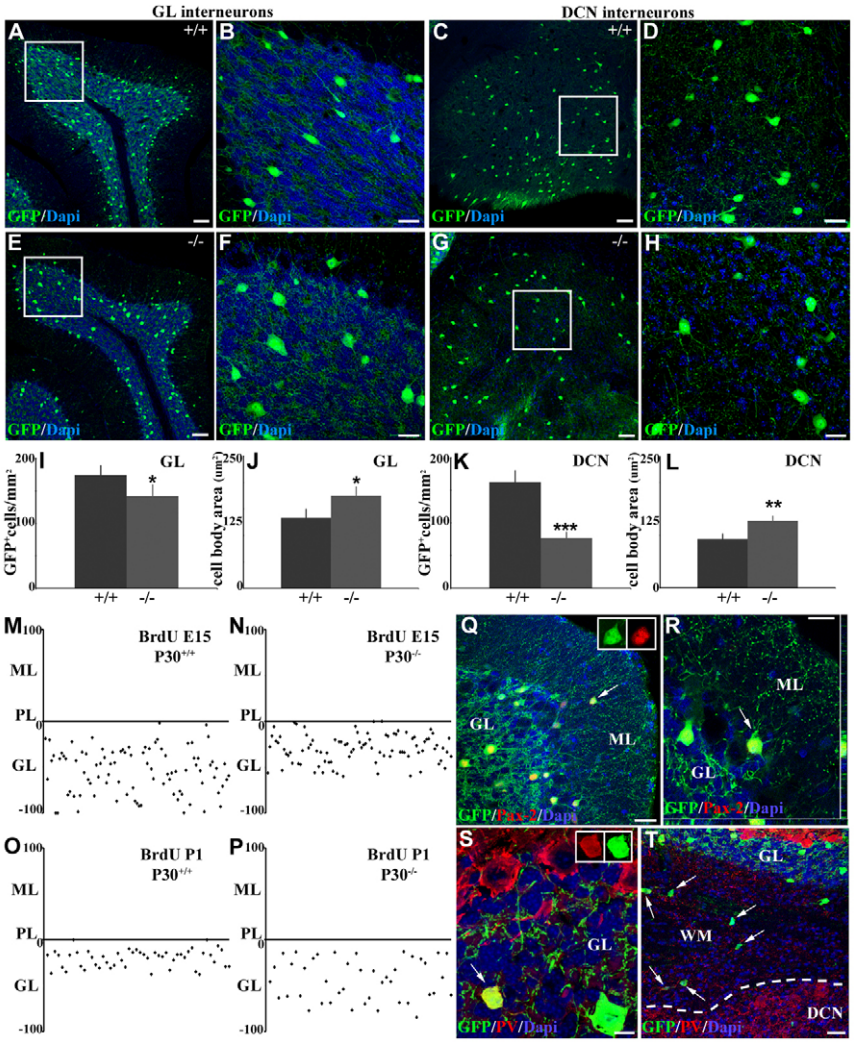

Fig. 3. Reduced numbers and oversized perikarya of GL and DCN interneurons in *Ccnd2*$^{-/-}$ cerebella. (**A-H**) Cerebellar sections from P30 Pax2/GFP (A-D) and Pax2/GFP/*Ccnd2*$^{-/-}$ (E-H) mice. In the mutant cerebella, both GL (A,B,E,F) and DCN (C,D,G,H) interneurons are reduced in number and display oversized somata. B,D,F,H are higher magnifications of the insets in A,C,E,G, respectively. (**I-L**) Quantification of interneuron density (I,K) and perikaryal size (J,L) in GL (I,J) and DCN (K,L). Data are mean+s.d. Student's *t*-test, **P*<0.01, ***P*<0.001, ****P*<0.0001. (**M-P**) Laminar positions of GL interneurons in wild-type and *Ccnd2*$^{-/-}$ mice that received BrdU injections at E15 (M,N) or P1 (O,P). Mutant interneurons show a reverse sequence of cortical placement. (**Q-T**) Ectopic interneurons in the P30 Pax2/GFP/*Ccnd2*$^{-/-}$ cerebellum: Pax2-positive Golgi cells in the ML (arrows in Q,R), PV-positive neurons in the GL (arrow in S) and DCN interneurons in the white matter surrounding the nuclear region (arrows in T). Insets in Q,J show individual immunofluorescence channels for the neurons indicated by arrows. ML, molecular layer; PL, Purkinje cell layer; GL, granular layer; WM, white matter; DCN, deep cerebellar nuclei. Scale bars: 60 μm in A,C,E,G; 30 μm in B,D,F,H,Q,T; 20 μm in R; 10 μm in S.

The reverse sequence of laminar positioning of mutant interneurons was suggestive of abnormal migration. This idea was corroborated by the presence of ectopically placed interneurons. In adult *Ccnd2*$^{-/-}$ cerebella, Golgi cells, identified by their size, dendritic morphology and strong expression of Pax2 protein in the adult (Maricich and Herrup, 1999), were found in the ML (Fig. 3Q,R; 6.7% of the whole Golgi cell population), whereas some small PV-immunopositive ML interneurons were misplaced in the GL (Fig. 3S; 5.4% of the whole ML interneuron population). Finally, ectopically positioned interneurons were scattered in the white matter surrounding the DCN region of mutant cerebella (Fig. 3T; 9.7% of the whole DCN interneuron population).

Cell cycle dynamics of PWM progenitors in *Ccnd2*$^{-/-}$ cerebella

In the embryonic cerebral cortex, loss of cyclin D2 modifies the duration of the G1 and S phases, leading to decreased proliferation and enhanced cell cycle exit of progenitors (Glickstein et al., 2009). Thus, we first evaluated the population of dividing progenitors in the PWM, visualized by Ki67 immunolabelling (Fig. 4A). At E15 and P1, the fraction of Ki67-positive cells was similar in wild-type and *Ccnd2*$^{-/-}$ mice. At P5, at the peak of ML interneuron production (Weisheit et al., 2006), the value was steady in mutant cerebella, whereas it was considerably higher in wild-type animals (Student's *t*-test, $P<0.0001$). Then, we compared the rate of incorporation of BrdU in PWM cells of wild-type and *Ccnd2*$^{-/-}$ cerebella 2 hours after administration of the nucleotide analogue at E15, P1 and P5 (Fig. 4B). In wild-type cerebella, the fraction of BrdU-labelled nuclei did not change between E15 and P1, but markedly increased at P5 (ANOVA with Bonferroni's Multiple Comparison Test, $P<0.0001$). In the mutant cerebella, equivalent values were obtained at E15 and P1, which were significantly higher than the corresponding ones of wild-type cerebella (Student's *t*-test; E15, $P=0.042$; P1, $P=0.022$). At P5, however, there was only a modest rise of BrdU-positive nuclei (ANOVA between E15, P1 and P5, $P=0.082$), and this value remained largely lower than that obtained from age-matched wild-type cerebella (Student's *t*-test, $P=0.0016$).

To determine the rate at which proliferating PWM cells continue to divide or leave the cycle, we pulsed BrdU at E15, P1 and P5, and examined the animals 24 hours later by double immunostaining for BrdU and Ki67 (Fig. 4C). In this material, BrdU-labelling highlights the population of dividing cells at the time of BrdU administration. Of these cells, those that are also stained by anti-Ki67 antibodies represent the 'proliferative' fraction that continue to divide 24 hours later (Glickstein et al., 2009). In the wild-type PWM, the 'proliferative' fraction significantly decreased between E15 and P1, and conspicuously increased at P5 (Fig. 4B; ANOVA with Bonferroni's Multiple Comparisons Test, $P<0.0001$). In *Ccnd2*$^{-/-}$ cerebella, the values remained steady at all

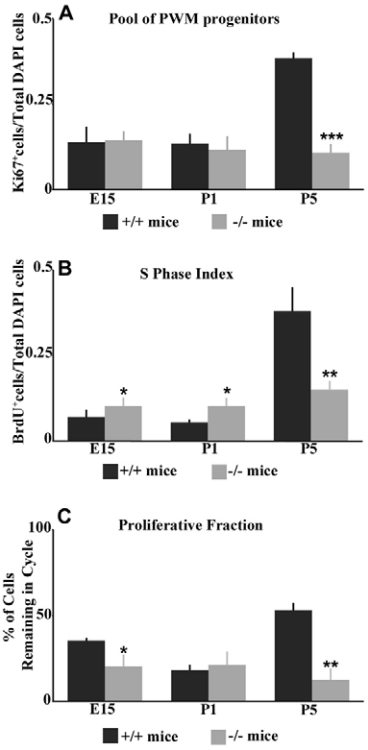

Fig. 4. Reduced proliferation and enhanced cell cycle exit of PWM progenitors in *Ccnd2*$^{-/-}$ mice. (**A**) Pool of dividing PWM progenitors (Ki67-positive cells/total number of DAPI-stained nuclei) observed in E15 SVZ, P1 and P5 PWM of wild-type and *Ccnd2*$^{-/-}$ mice. (**B**) S-phase index (BrdU-positive nuclei/total number of DAPI-stained nuclei) was calculated in the same regions of wild-type and mutant mice 2 hours after the BrdU administration at E15, P1 and P5. (**C**) Proliferative fraction (percentage of cells double-labelled for Ki67 and BrdU/total number of BrdU-positive cells 24 hours after BrdU pulse) represents the cells that continued to divide 24 hours after BrdU pulse at E15, P1 and P5. Data are mean+s.d. Student's *t*-test, **P*<0.05, ***P*<0.005, *P*<0.0005 (wild type versus *Ccnd2*$^{-/-}$ at the same time-point; see text for additional tests and parameters).

ages (ANOVA, *P*=0.29), and were significantly lower than those obtained from wild-type mice at E15 and P5 (Student's *t*-test, E15, *P*=0.022; P5, *P*=0.0009).

Delayed maturation and migration of postmitotic interneurons in *Ccnd2*$^{-/-}$ cerebella

The progenitors of cerebellar GABAergic interneurons upregulate Pax2 at the time of their last mitosis. Thereafter, the young postmitotic interneurons, which retain Pax2 expression throughout their differentiation, sojourn in the PWM for up to several days, before moving to their final destination (Leto et al., 2009). At E15, the number of Pax2 positive cells/mm^2 in the SVZ was slightly, though not significantly, higher in *Ccnd2*$^{-/-}$ than in wild-type mice (Fig. 5A; Student's *t*-test, *P*=0.352), whereas a reversed situation was observed in the PWM at P1 (Fig. 5A; Student's *t*-test, *P*=0.121). At P5, however, the number of Pax2-positive cells/mm^2 of PWM was significantly higher in wild type than in mutant cerebella (Fig. 5A; Student's *t*-test, *P*<0.0001). To determine whether the schedule of interneuron maturation was altered in *Ccnd2*$^{-/-}$ mice, we pulsed BrdU at P3 and killed the animals at different time intervals (Fig. 5B-G; parallel experiments in which BrdU was injected at P1 or P5 yielded similar results – not shown). In wild-type cerebella (Fig. 5B), Pax-2/BrdU double-labelled nuclei were already observed at 2 hours, when they were mostly localized in the PWM. One and three days later, double-labelled cells appeared in the cortical layers, consistent with the progressive migration of young interneurons (Fig. 5B,D). Strikingly, in *Ccnd2*$^{-/-}$ cerebella, the first Pax-2/BrdU double-labelled nuclei were only observed 72 hours after administration of the nucleotide analogue, and they were almost exclusively confined within the PWM (Fig. 5C,E,F). Accordingly, Pax2 staining intensity of these mutant nuclei was considerably fainter than that of their age-matched wild-type counterparts (Fig. 5G, Student's *t*-test, *P*<0.0001). Pax2-positive/BrdU-retaining nuclei were eventually detected in the cortical layers of the mutant cerebella at longer intervals after BrdU pulse, but many of such cells were still in the PWM at the longest times examined (5 days, Fig. 5H,I; 8 days, Fig. 5J,K).

Given the delayed onset of Pax2 expression in *Ccnd2*$^{-/-}$ cerebella, we applied anti-Sox2 antibodies to visualize progenitors in the PWM (see Fig. S2A-F in the supplementary material). Two hours after BrdU pulse, BrdU/Sox2 double-stained nuclei were present in both wild-type and mutant cerebella, but there were no Pax2/Sox2 double-labelled nuclei (see Fig. S2G-L in the supplementary material), indicating that Sox2 cannot be used to reveal interneuron progenitors prior of Pax2 upregulation.

To evaluate the possible contribution of cell death to the reduction of interneuron numbers (Huard et al., 1999), we quantified the density of caspase 3-immunopositive cells in the PWM at P1 and P5 (see Fig. S3A,B,D,E in the supplementary material). At both ages, the number of immunolabelled cells was moderately higher in mutant mice, but these differences were not significant (see Fig. S3C,F in the supplementary material; results are ±s.d.: P1, *Ccnd2*$^{-/-}$, 47±10.4 cells/mm^2; wild type, 32±5.2 cells/mm^2; Student's *t*-test, *P*=0.089; P5, *Ccnd2*$^{-/-}$, 38±5.2 cells/mm^2, wild type 29±4.8 SD cells/mm^2, Student's *t*-test, *P*=0.093).

GABAergic interneuron defects in *Ccnd2*$^{-/-}$ cerebella are cell autonomous

To elucidate the relative contribution of cell-autonomous processes and environmental constraints to the phenotype of *Ccnd2*$^{-/-}$ interneurons, we performed homo/heterochronic transplantation experiments. Cells from P7 Pax2/GFP wild-type cerebella were grafted to P1 or P7 wild-type or mutant hosts, and their fate was assessed 1 month later. Donor cells implanted in wild-type cerebella adopted host-specific phenotypes and laminar positions (Fig. 6A,C,D,F), and the same result was obtained when these wild-type donors were exposed to the mutant environment (Fig. 6B,C,E,F). In both P1 and P7 hosts, the phenotypic repertoires and laminar distributions acquired by interneurons grafted to wild-type or *Ccnd2*$^{-/-}$ cerebella were not different (Fig. 6C,F; Student's *t*-test for the positions of cells transplanted to *Ccnd2*$^{-/-}$ versus wild-type cerebella; P1 host, *P*=0.164; P7 host, *P*=0.475), although there was a tendency for a more superficial localization of cells grafted to the mutant ML (Fig. 6C). The latter cells consistently displayed typical phenotypes of ML interneurons, with no sign of ectopic homing of GL interneurons in the recipient ML. Notably, however, in the mutant cerebella, the perikarya of donor interneurons were larger than their counterparts implanted in wild-type recipients (*Ccnd2*$^{-/-}$ host, 62.3±15.8 mm^2, *n*=115; wild-type host, 42.9±17.5 mm^2, *n*=78; Student's *t*-test, *P*<0.0001) and displayed extensive neuritic arbours (compare Fig. 6A,D with 6B,E).

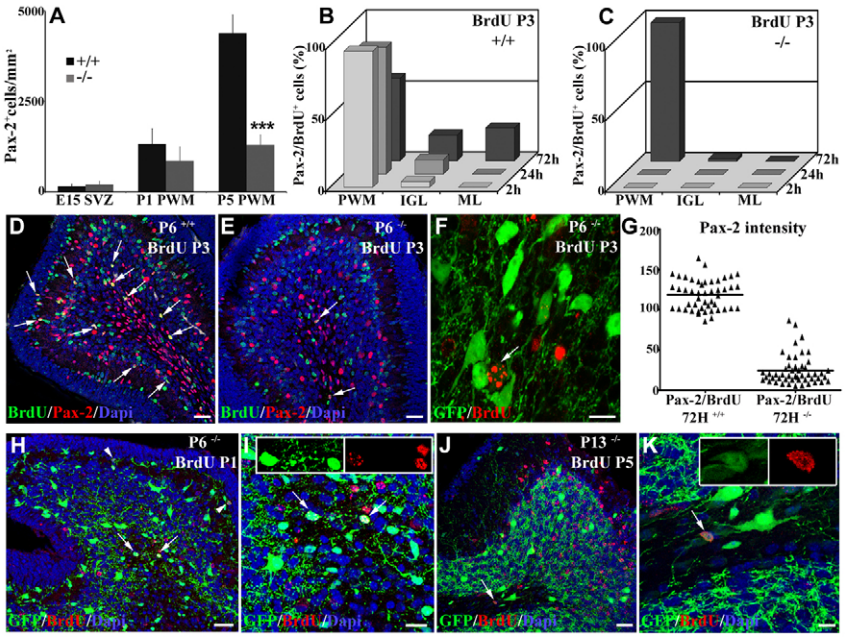

Fig. 5. Delayed maturation and migration of *Ccnd2*$^{-/-}$ inhibitory interneurons. (**A**) Density of Pax2-positive cells in the E15 SVZ and in the P1 and P5 PWM of wild-type and *Ccnd2*$^{-/-}$ mice. Data are mean+s.d. (**B**,**C**) Frequency of Pax2/BrdU double-labelled cells in PWM and cortical layers, 2 hours, 24 hours and 72 hours after BrdU pulse to P3 wild-type (B) and *Ccnd2*$^{-/-}$ (C) mice. Student's *t*-test, ***P<0.0001. (**D-F**) Three days after BrdU pulse, Pax2/BrdU double-labelled wild-type interneurons are located in the cortex (arrows in D), whereas their mutant counterparts are still in the PWM (arrows in E,F). (**G**) Quantification of Pax2/GFP fluorescence intensity in cells double-labelled for Pax2/GFP and BrdU of wild-type and *Ccnd2*$^{-/-}$ mice 72 hours after BrdU pulse at P3. (**H-K**) Five days after BrdU injection at P1 (arrows in H,I) or 8 days after incorporation of the nucleotide analogue at P5 (arrows in J,K), mutant interneurons, double-labelled for Pax2 and BrdU, are still located in the PWM (arrowheads in H indicate interneurons that migrated to the cortex). Insets in I,K show individual immunofluorescence channels for the neurons indicated by arrows. PWM, prospective white matter; IGL, internal granular layer; ML, molecular layer. Scale bars: 30 μm in D,E,H,J; 15 μm in I; 10 μm in F,K.

In a second series of experiments, GFP-tagged wild-type or *Ccnd2*$^{-/-}$ cells were isolated at different embryonic and postnatal ages, and homo/heterochronically grafted to wild-type recipients (see Table S2 in the supplementary material). Seven days later, immature mutant interneurons were detected at the ML-EGL interface (Fig. 7A), indicating that at least some *Ccnd2*$^{-/-}$ cells were able to follow the typical migratory route of cerebellar interneurons. At 30 days, even though the number of surviving *Ccnd2*$^{-/-}$ donors was always low, many transplanted interneurons displayed typical phenotypic traits and settled in canonical cortical positions (e.g. Fig. 7B,C). Nonetheless, when entire populations of donor cells were compared, the laminar placement of mutant cells in the recipient cortex was significantly deeper than that of their wild-type counterparts in age-matched grafts (Fig. 7D; Student's *t*-test between the positions of P7 donor knockout versus wild-type cells in P7 cerebella, P=0.02). In addition, whereas wild-type donors invariably acquired typical phenotypes and positions (not shown) (Leto et al., 2009), numerous mutant interneurons were clearly ectopic, such as Golgi neurons misplaced in the ML (Fig. 7E-I), or displayed abnormal features, including inverted orientation (Fig. 7G) or hybrid morphological traits (Fig. 7H,I).

To reveal possible cell cycle-independent effects of cyclin D2 loss, we grafted P7 *Ccnd2*$^{-/-}$ Pax2/GFP cells to age-matched wild-type cerebella and pulsed BrdU 2 hours after transplantation, to visualize donor cells that proliferate in the recipient environment. One month later, we failed to detect any *Ccnd2*$^{-/-}$ interneurons that had incorporated BrdU (Fig. 7J-L), indicating that virtually all donor interneurons originate from postmitotic cells. However, the cortical placement of these cells in the ML was deeper than that of both postmitotic and dividing wild-type cells transplanted in the same conditions (Student's *t*-test, P<0.0001 in both cases). Thus, the aberrant laminar fate of donor mutant cells does not depend on whether they proliferate in the recipient environment.

DISCUSSION

To determine whether cyclin D2 is required for the generation of specific interneuron subtypes, we compared the genesis of cerebellar GABAergic interneurons in wild-type and *Ccnd2*$^{-/-}$ mice. We found that loss of cyclin D2 function disrupts the whole process of interneuron ontogenesis. The mutant cerebellum is characterized by abnormal proliferation rates of PWM progenitors, consistent with the distribution of cyclin D2 expression in wild-type cerebella. The generation of inhibitory interneurons is reduced and their maturation and migration are delayed, leading to aberrant homing in the cortical layers. These abnormalities become more severe during postnatal development, when ML interneurons are generated. Furthermore, transplantation experiments show that the peculiar traits of mutant interneurons are largely determined by cell-autonomous mechanisms. Together, these observations indicate that cyclin D2 is not required for neuronal specification and

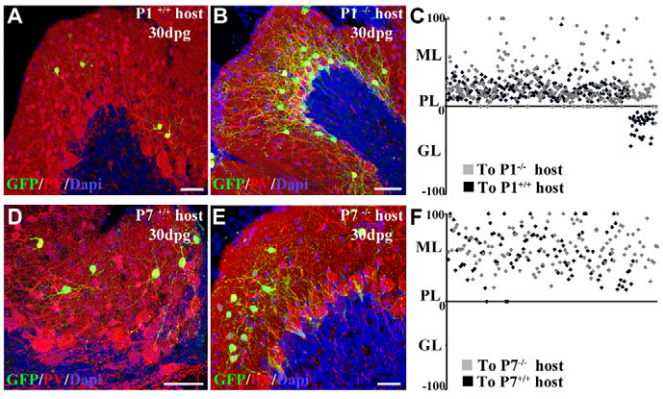

Fig. 6. Normal development of wild-type interneurons transplanted to *Ccnd2*$^{-/-}$ cerebella. (**A-C**) Heterochronic transplantation of P7 Pax2/GFP cells into P1 wild-type (A) and *Ccnd2*$^{-/-}$ (B) cerebella: in both recipients, donor cells (green) generate mature ML interneurons, preferentially placed in the innermost part of the layer (C). (**D-F**) P7 Pax2/GFP cells (green) homochronically grafted to wild-type (D) and *Ccnd2*$^{-/-}$ (E) hosts produce ML interneurons scattered at different levels of the layer (F). ML, molecular layer; PL, Purkinje cell layer; GL, granular layer; dpg, days post graft. Scale bars: 30 μm in A,E; 50 μm in B; 40 μm in D.

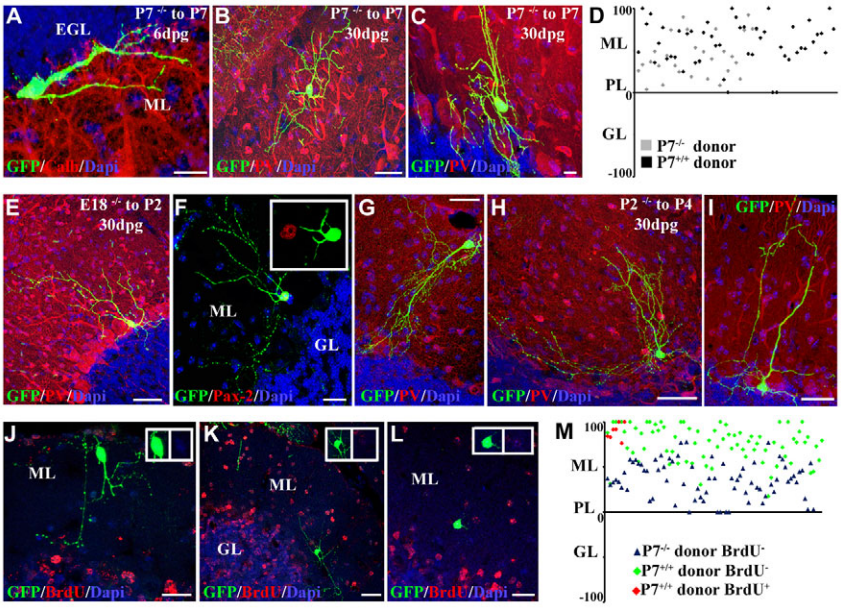

Fig. 7. Fate of *Ccnd2*$^{-/-}$ interneurons grafted to wild-type cerebella. (**A**) Seven days after homochronic transplantation, a P7 Pax2/GFP/*Ccnd2*$^{-/-}$ donor cell (green) has reached the ML-EGL border. (**B-D**) One month after transplantation, donor cells adopt mature phenotypes of stellate (B) and basket (C) interneurons. (D) Laminar distribution of P7 wild-type and *Ccnd2*$^{-/-}$ donor interneurons grafted to P7 wild-type cerebella: mutant cells are located deeper in the host ML than their wild-type counterparts. (**E-G**) Examples of Golgi neurons ectopically positioned in the ML (E18 *Ccnd2*$^{-/-}$ donors transplanted to P2 wild-type host, examined at P30). The grafted neuron shown in G also has an inverted orientation. Inset in F show individual flurescence channels. (**H**,**I**) Ectopic position in the host ML and hybrid morphology of presumptive Golgi neurons derived from mutant donors (P2 *Ccnd2*$^{-/-}$ donors transplanted to P4 wild-type host, examined at P30). (**J-L**) Examples of P7 Pax2/GFP/*Ccnd2*$^{-/-}$ donor cells transplanted to homochronic wild-type recipients that received a single BrdU pulse 2 hours after transplantation. Insets show individual fluorescence channels. (**M**) Laminar distribution of BrdU-labelled or unlabelled P7 wild-type and mutant donor cells grafted to homochronic wild-type hosts. EGL, external granular layer; ML, molecular layer; PL, Purkinje cell layer; GL, granular layer; dpg, days post graft. Scale bars: 10 μm in A,C; 20 μm in J,L; 30 μm in B,F,G,I,K; 40 μm in H,E.

phenotype acquisition, but plays a crucial function in regulating the production and the number of interneurons belonging to different categories.

Loss of cyclin D2 function affects all types of cerebellar interneurons

Huard et al. (Huard et al., 1999) proposed that *Ccnd2*$^{-/-}$ mice are affected by selective loss of stellate cells, because neurons in the ML (but not in the GL) are severely reduced in number, and basket axon pinceaux still enwrap Purkinje cell perikarya. These findings suggest that cyclin D2 is needed for the generation or differentiation of specific interneuron phenotypes. However, basket and stellate cells are thought to belong to a single class of interneurons, who acquire distinctive traits under the influence of local cues in the ML (Rakic, 1972; Sultan and Bower, 1998). In particular, the powerful guidance mechanisms that attracts the axons of ML interneurons towards Purkinje cell perikarya (Ango et al., 2004; Sotelo, 2008) probably favour the acquisition of basket cell features, the pinceaux, by the sparse interneurons that populate the *Ccnd2*$^{-/-}$ ML.

Our observations show that all types of interneurons, including stellate cells, are present in the mutant cerebellum, but all interneuron populations are reduced, although to different extents. Furthermore, *Ccnd2*$^{-/-}$ interneurons are larger than their wild-type counterparts and bear extensive dendritic and axonal arbours. The latter features are also developed by wild-type interneurons exposed to the mutant environment. Oversized cell bodies and neuritic arbours are typical of conditions such as partial neuronal degeneration, in which spared neurons expand their neuritic fields to compensate for the loss of innervation (Purves, 1988; Neppi-Modona et al., 1999). Accordingly, *Ccnd2*$^{-/-}$ interneurons that reach maturity behave as healthy cells, capable of making contact with enlarged populations of potential partners. Thus, cyclin D2 appears to be crucial for determining the quantity rather than the quality of cerebellar interneurons.

Cyclin D2 regulates the amplification of PWM progenitors

Upon mitogen stimulation, D-type cyclins dimerize and activate specific cyclin-dependent kinases to control G1 phase progression (Sherr, 1995; Sherr and Roberts, 1999). The duration of cell cycle, and notably of G1 phase, determines the balance between expansion of progenitor pools and neuronal differentiation (Salomoni and Calegari, 2010). For example, during corticogenesis, cell cycle length varies in space and time to match specific neurogenic requirements (Lukaszewicz et al., 2005; Caviness et al., 2009). This regulation is impaired after loss of cyclin D2. In the developing neocortex, cyclin D1 is expressed in the VN, whereas cyclin D2 is active in intermediate progenitors of SVZ (Glickstein et al., 2007a). Loss of *Ccnd2*$^{-/-}$ function, which is not compensated for by ectopic upregulation of cyclin D1, hampers the expansion of the latter progenitors by lengthening the G1 phase and favouring cell cycle exit (Glickstein et al., 2009). Consequently, the generation of inhibitory interneurons is defective (Glickstein et al., 2007b).

In the cerebellum, the two cyclins also show a complementary distribution. Cyclin D2 is primarily expressed in SVZ and PWM, and it is not replaced by other cyclins (Ciemerych et al., 2002). The

progenitors of cerebellar interneurons divide in the PWM, where they are exposed to environmental signals that direct the sequential generation of different mature types (Carletti and Rossi, 2008; Leto et al., 2010). In this process, the proliferation rates of progenitors must be finely modulated at different ontogenetic stages to produce interneuron subpopulations of desired sizes. Accordingly, in wild-type animals there is a brisk amplification of PWM precursors during the postnatal period when ML interneurons are generated. Cyclin D2 is an essential element of this mechanism.

Because of the lack of a selective marker to visualize interneuron progenitors, we could only evaluate proliferation parameters on the whole population of dividing cells in the PWM, which is heterogeneous (Lee et al., 2005; Grimaldi et al., 2009; Silbereis et al., 2009). Nonetheless, the results were clear. Up to P1, the proliferation rates of *Ccnd2*$^{-/-}$ cells were comparable with (and even slightly faster than) those of age-matched wild-type cerebella. Accordingly, the populations of interneurons produced during this period were moderately reduced. After birth, mutant progenitors failed to accelerate their mitotic pace and showed increased propensity to leave the cycle. As a consequence, the pool of proliferating cells was precociously exhausted and the production of ML interneurons dramatically dampened. The final number of interneurons could be also influenced by increased rates of cell death (Huard et al., 1999). Our observations, however, indicate that such a mechanism does not contribute significantly to the mutant phenotype.

The activity of cyclin D2, and the ensuing regulation of proliferation rates and neuronal production, is under control of environmental signals. Transplantation of cerebellar cells of a defined age yields more interneurons in postnatal than in embryonic recipients (Leto et al., 2006), suggesting that the former environment provides cues to expand the progenitor pool. Among such cues, potential candidates include basic fibroblast growth factor, which stimulates the proliferation of PWM cells (Lee et al., 2005). In addition, cyclin D2 is a direct transcriptional target of sonic hedgehog (Shh) signalling (Simpson et al., 2009; Vaillant and Monard, 2009). The effects of Shh on the cyclin D2-expressing PWM cells are still unknown. However, Shh potently stimulates the proliferation in the EGL (Dahmane and Ruiz i Altaba, 1999; Wallace, 1999; Wechsler-Reya and Scott, 1999) and in the VN, which is the origin of all cerebellar GABAergic neurons (Huang et al., 2010). Finally, cyclin D2 expression in the cerebellum is driven by thyroid hormones (Poguet et al., 2003). In rodents, these hormones influence cell growth and differentiation during postnatal cerebellar development (Koibuchi, 2008), and, notably, they promote the proliferation and maturation of GABAergic interneurons (Manzano et al., 2007).

Cyclin D2 regulates the maturation rhythm of cerebellar interneurons

Loss of cyclin D2 function also impaired the differentiation of cerebellar interneurons. The maturation of juvenile interneurons in the PWM, evidenced by Pax2 upregulation, was severely delayed. Moreover, migratory processes were dramatically slowed down, and the typical inside-out sequence of laminar placement was reversed. It is difficult to relate these effects directly to cyclin D2-mediated regulation of mitotic activity. It is possible that the abnormal length of the G1 phase, which is crucial to secure appropriate exposure of the cell to fate-determining factors (Salomoni and Calegari, 2010), may impair the ability of the postmitotic neuron to carry out its ontogenetic program on schedule. Laminar fate and acquisition of mature traits are temporally related to the birthdate of cerebellar interneurons (Leto et al., 2009; Leto et al., 2010), highlighting the relevance of events occurring at the time of the last cell division. As a consequence, mutant cells may be unable to respond appropriately to spatio-temporally patterned environmental signals that direct their migration and differentiation. A mismatch between the rhythm of cell maturation and the ontogenetic evolution of the surrounding milieu could impair interneuron migration (Cameron et al., 2009), leading to a reverse sequence of laminar homing or ectopic placement. Transplantation experiments show that the mutant cerebellum is fully receptive and supportive to wild-type cells, showing that the abnormalities of *Ccnd2*$^{-/-}$ interneurons are exclusively due to their intrinsic inability to follow otherwise efficient extrinsic cues. However, the observation that postmitotic *Ccnd2*$^{-/-}$ donor cells are abnormally positioned suggests that the mutant interneuron phenotypes could be also produced by a cell cycle-independent effect, as recently proposed for cyclin D1 (Zhong et al., 2010). In any case, the presence of all the types of GABAergic interneurons in the mutant cerebellum indicates that, although cyclin D2 function is required to keep normal maturation schedules, it does not impair the ability for acquiring fully mature morphological phenotypes.

The analysis of *Ccnd2*$^{-/-}$ cerebella indicates that fine-tuning of cell cycle in SVZ and PWM is crucial to modulate the proliferation rates of progenitors and the ensuing maturation of young interneurons. The mechanism is particularly fragile when mitotic activity must be briskly accelerated to increase production. ML interneurons, which largely outnumber all the other types (Altman and Bayer, 1997), are produced during a postnatal period that has about the same duration as the embryonic time-window when GL and DCN interneurons are born (Leto et al., 2006; Leto et al., 2009). As a consequence, the mutant progenitors, which manage to maintain the required pace during embryonic life, dramatically fail after birth when huge quantities of ML interneurons must be generated within a short time. On the whole, these findings indicate that fine modulation of cell cycle dynamics is required to generate appropriate numbers of interneurons at due times. Cell cycle regulation may also influence the migration and differentiation of interneurons. Concerning the latter processes, however, cell cycle-independent roles of cyclin D2 cannot be excluded.

Acknowledgements
This work was supported by grants from Ministero dell'Università e della Ricerca (PRIN 2007 prog. nr. 2007F7AJYJ), from Compagnia di San Paolo (Neurotransplant Project 2008; GABAGEN project 2009), from Regione Piemonte (Project A14/05; Ricerca Sanitaria Finalizzata, 2009) and from Ataxia UK. K.L. is supported by a fellowship from Compagnia di San Paolo.

Competing interests statement
The authors declare no competing financial interests.

Supplementary material
Supplementary material for this article is available at
http://dev.biologists.org/lookup/suppl/doi:10.1242/dev.064379/-/DC1

References

Abercrombie, M. (1946). Estimation of nuclear populations from microtome sections. *Anat. Rec.* **94**, 239-247.
Altman, J. and Bayer, S. A. (1997). *Development of the Cerebellar System in Relation to its Evolution, Structures and Functions.* Boca Raton, FL: CRC.
Ango, F., di Cristo, G., Higashiyama, H., Bennett, V., Wu, P. and Huang, Z. J. (2004). Ankyrin-based subcellular gradient of neurofascin, an immunoglobulin family protein, directs GABAergic innervation at purkinje axon initial segment. *Cell* **119**, 257-272.
Bastianelli, E. (2003). Distribution of calcium-binding proteins in the cerebellum. *Cerebellum* **2**, 242-262.
Cameron, D. B., Kasai, K., Jiang, Y., Hu, T., Saeki, Y. and Komuro, H. (2009). Four distinct phases of basket/stellate cell migration after entering their final destination (the molecular layer) in the developing cerebellum. *Dev. Biol.* **332**, 309-324.

Carletti, B. and Rossi, F. (2008). Neurogenesis in the cerebellum. *Neuroscientist* **14**, 91-100.
Carletti, B., Grimaldi, P., Magrassi, L. and Rossi, F. (2002). Specification of cerebellar progenitors following heterotopic/heterochronic transplantation to the embryonic CNS *in vivo* and *in vitro*. *J. Neurosci.* **22**, 7132-7146.
Caviness, V. S., Jr, Nowakowski, R. S. and Bhide, P. G. (2009). Neocortical neurogenesis: morphogenetic gradients and beyond. *Trends Neurosci.* **32**, 443-450.
Celio, M. R. (1990). Calbindin D-28k and parvalbumin in the rat nervous system. *Neuroscience* **32**, 375-475.
Ciemerych, M. A., Kenney, A. M., Sicinska, E., Kalaszczynska, I., Bronson, R. T., Rowitch, D. H., Gardner, H. and Sicinski, P. (2002). Development of mice expressing a single D-type cyclin. *Genes Dev.* **16**, 3277-3289.
Dahmane, N. and Ruiz i Altaba, A. (1999). Sonic hedgehog regulates the growth and patterning of the cerebellum. *Development* **126**, 3089-3100.
Glickstein, S. B., Alexander, S. and Ross, M. E. (2007a). Differences in cyclin d2 and d1 protein expression distinguish forebrain progenitor subsets. *Cereb. Cortex* **17**, 632-642.
Glickstein, S. B., Moore, H., Slowinska, B., Racchumi, J., Suh, M., Chuhma, N. and Ross, M. E. (2007b). Selective cortical interneuron and GABA deficits in cyclin D2-null mice. *Development* **134**, 4083-4093.
Glickstein, S. B., Monaghan, J. A., Koeller, H. B., Jones, T. K. and Ross, M. E. (2009). Cyclin D2 is critical for intermediate progenitor cell proliferation in the embryonic cortex. *J. Neurosci.* **29**, 9614-9624.
Grimaldi, P., Parras, C., Guillemot, F., Rossi, F. and Wassef, M. (2009). Origins and control of the differentiation of inhibitory interneurons and glia in the cerebellum. *Dev. Biol.* **328**, 422-433.
Huang, X., Liu, J., Ketova, T., Fleming, J. T., Grover, V. K., Cooper, M. K., Litingtung, Y. and Chiang, C. (2010). Transventricular delivery of Sonic hedgehog is essential to cerebellar ventricular zone development. *Proc. Natl. Acad. Sci. USA* **107**, 8422-8427.
Huard, J. M., Forster, C. C., Carter, M. L., Sicinski, P. and Ross, M. E. (1999). Cerebellar histogenesis is disturbed in mice lacking cyclin D2. *Development* **126**, 1927-1935.
Jankovski, A., Rossi, F. and Sotelo, C. (1996). Neuronal precursors in the postnatal mouse cerebellum are fully committed cells: evidence from heterochronic transplantation. *Eur. J. Neurosci.* **8**, 2308-2320.
Koibuchi, N. (2008). The role of thyroid hormone on cerebellar development. *Cerebellum* **7**, 530-533.
Lee, A., Kessler, J. D., Read, T. A., Kaiser, C., Corbeil, D., Huttner, W. B., Johnson, J. E. and Wechsler-Reya, R. J. (2005). Isolation of neural stem cells from the postnatal cerebellum. *Nat. Neurosci.* **6**, 723-729.
Lee, J., Go, Y., Kang, I., Han, Y. M. and Kim, J. (2010). Oct-4 controls cell-cycle progression of embryonic stem cells. *Biochem. J.* **426**, 171-181.
Leto, K., Carletti, B., Williams, I. M., Magrassi, L. and Rossi, F. (2006). Different types of cerebellar GABAergic interneurons originate from a common pool of multipotent progenitor cells. *J. Neurosci.* **26**, 11682-11694.
Leto, K., Bartolini, A., Yanagawa, Y., Obata, K., Magrassi, L., Schilling, K. and Rossi, F. (2009). Laminar fate and phenotype specification of cerebellar GABAergic interneurons. *J. Neurosci.* **29**, 7079-7091.
Leto, K., Bartolini, A. and Rossi, F. (2010). The prospective white matter: an atypical neurogenic niche in the developing cerebellum. *Arch. Ital. Biol.* **148**, 137-146.
Lukaszewicz, A., Savatier, P., Cortay, V., Giroud, P., Huissoud, C., Berland, M., Kennedy, H. and Dehay, C. (2005). G1 phase regulation, area-specific cell cycle control, and cytoarchitectonics in the primate cortex. *Neuron* **47**, 353-364.
Machold, R. and Fishell, G. (2005). Math1 is expressed in temporally discrete pools of cerebellar rhombic-lip neural progenitors. *Neuron* **48**, 17-24.
Manzano, J., Cuadrado, M., Morte, B. and Bernal, J. (2007). Influence of thyroid hormone and thyroid hormone receptors in the generation of cerebellar gamma-aminobutyric acid-ergic interneurons from precursor cells. *Endocrinology* **148**, 5746-5751.
Maricich, S. M. and Herrup, K. (1999). Pax-2 expression defines a subset of GABAergic interneurons and their precursors in the developing murine cerebellum. *J. Neurobiol.* **41**, 281-294.
Milosevich, A. and Goldman, J. E. (2002). Progenitors in the postnatal cerebellar white matter are antigenically heterogeneous. *J. Comp. Neurol.* **452**, 192-203.
Mizuhara, E., Minaki, Y., Nakatani, T., Kumai, M., Inoue, T., Muguruma, K., Sasai, Y. and Ono, Y. (2010). Purkinje cells originate from cerebellar ventricular zone progenitors positive for Neph3 and E-cadherin. *Dev. Biol.* **338**, 202-214.
Neppi-Modona, M., Rossi, F. and Strata, P. (1999). Phenotype changes of inferior olive neurons following collateral reinnervation. *Neuroscience* **94**, 209-215.
Pfeffer, P. L., Payer, B., Reim, G., di Magliano, M. P. and Busslinger, M. (2002). The activation and maintenance of Pax-2 expression at the mid-hindbrain boundary is controlled by separate enhancers. *Development* **129**, 307-318.
Poguet, A. L., Legrand, C., Feng, X., Yen, P. M., Meltzer, P., Samarut, J. and Flamant, F. (2003). Microarray analysis of knockout mice identifies cyclin D2 as a possible mediator for the action of thyroid hormone during the postnatal development of the cerebellum. *Dev. Biol.* **254**, 188-199.
Purves, D. (1988). *Body and Brain*. Sunderland: Sinauer.
Rakic, P. (1972). Extrinsic cytological determinants of basket and stellate cell dendritic pattern in the cerebellar molecular layer. *J. Comp. Neurol.* **146**, 335-354.
Sakagami, K., Gan, L. and Yang, X. J. (2009). Distinct effects of Hedgehog signaling on neuronal fate specification and cell cycle progression in the embryonic mouse retina. *J. Neurosci.* **29**, 6932-6944.
Salomoni, P. and Calegari, F. (2010). Cell cycle control of mammalian neural stem cells: putting a speed limit on G1. *Trends Cell Biol.* **20**, 233-243.
Sessa, A., Mao, C. A., Hadjantonakis, A. K., Klein, W. H. and Broccoli, V. (2008). Tbr2 directs conversion of radial glia into basal precursors and guides neuronal amplification by indirect neurogenesis in the developing neocortex. *Neuron* **60**, 56-69.
Sherr, C. J. (1995). Mammalian G1 cyclins and cell cycle progression. *Proc. Assoc. Am. Physicians* **107**, 181-186.
Sherr, C. J. and Roberts, J. M. (1999). CDK inhibitors: positive and negative regulators of G1-phase progression. *Genes Dev.* **13**, 1501-1512.
Sicinski, P., Donaher, J. L., Parker, S. B., Li, T., Fazeli, A., Gardner, H., Haslam, S. Z., Bronson, R. T., Elledge, S. J. and Weinberg, R. A. (1995). Cyclin D1 provides a link between development and oncogenesis in the retina and breast. *Cell* **82**, 621- 630.
Sicinski, P., Donaher, J. L., Geng, Y., Parker, S. B., Gardner, H., Park, M. Y., Robker, R. L., Richards, J. S., McGinnis, L. K., Biggers, J. D. et al. (1996). Cyclin D2 is an FSH-responsive gene involved in gonadal cell proliferation and oncogenesis. *Nature* **384**, 470-474.
Silbereis, J., Cheng, E., Ganat, Y. M., Ment, L. R. and Vaccarino, F. M. (2009). Precursors with glial fibrillary acidic protein promoter activity transiently generate GABA interneurons in the postnatal cerebellum. *Stem Cells* **27**, 1152-1163.
Simpson, F., Kerr, M. C. and Wicking, C. (2009). Trafficking, development and hedgehog. *Mech. Dev.* **126**, 279-288.
Sotelo, C. (2008). Development of "Pinceaux" formations and dendritic translocation of climbing fibers during the acquisition of the balance between glutamatergic and gamma-aminobutyric acidergic inputs in developing Purkinje cells. *J. Comp. Neurol.* **506**, 240-262.
Sultan, F. and Bower, J. M. (1998). Quantitative Golgi study of the rat cerebellar molecular layer interneurons using principal components analysis. *J. Comp. Neurol.* **393**, 353-373.
Vaillant, C. and Monard, D. (2009). SHH pathway and cerebellar development. *Cerebellum* **8**, 291-301.
Wallace, V. A. (1999). Purkinje-cell-derived Sonic hedgehog regulates granule neuron precursor cell proliferation in the developing mouse cerebellum. *Curr. Biol.* **9**, 445-448.
Wang, V. Y., Rose, M. F. and Zoghbi, H. (2005). Math1 expression redefines the rhombic lip derivatives and reveals novel lineages within the brainstem and cerebellum. *Neuron* **48**, 31- 43.
Wechsler-Reya, R. J. and Scott, M. P. (1999). Control of neuronal precursor proliferation in the cerebellum by Sonic Hedgehog. *Neuron* **22**, 103-114.
Weisheit, G., Gliem, M., Endl, E., Pfeffer, P. L., Busslinger, M. and Schilling, K. (2006). Postnatal development of the murine cerebellar cortex: formation and early dispersal of basket, stellate and Golgi neurons. *Eur. J. Neurosci.* **24**, 466-478.
Zhang, L. and Goldman, J. E. (1996). Generation of cerebellar interneurons from dividing progenitors in white matter. *Neuron* **16**, 47-54.
Zhong, Z., Yeow, W. S., Zou, C., Wassell, R., Wang, C., Pestell, R. G., Quong, J. N. and Quong, A. A. (2010). Cyclin D1/cyclin-dependent kinase 4 interacts with filamin A and affects the migration and invasion potential of breast cancer cells. *Cancer Res.* **70**, 2105-2114.
Zordan, P., Croci, L., Hawkes, R. and Consalez, G. G. (2008). Comparative analysis of proneural gene expression in the embryonic cerebellum. *Dev. Dyn.* **237**, 1726-1735.